Journal of Applied Polymer Science

Effect of clay type on dispersion and barrier properties of hydrophobically modified poly(vinyl alcohol)–bentonite nanocomposites

Caisa Johansson,[1] Francis Clegg[2]

[1]Karlstad University, Faculty of Health, Science and Technology, Department of Engineering and Chemical Sciences, SE-651 88 Karlstad, Sweden

[2]Materials and Engineering Research Institute, Sheffield Hallam University, Howard Street, Sheffield S1 1WB, United Kingdom

Correspondence to: C. Johansson (E-mail: caisa.johansson@kau.se)

ABSTRACT: The oxygen and water vapor permeability at high relative humidity was studied for composite films formed by incorporation of three different bentonites (MMT) into an ethylene-modified, water-soluble poly(vinyl alcohol), EPVOH. The oxygen permeability decreased linearly with an increased addition of hydrophilic MMTs. X-ray diffraction and Fourier transform infrared spectroscopy suggested a homogeneous distribution in the thickness direction with disordered and probably exfoliated structures for hydrophilic MMTs. In contrast, organophilic modified clay showed an intercalated structure with the clay preferentially located at the lower film surface, a combination which was however efficient in reducing the water vapor- and oxygen permeabilities at low addition levels. Composite films of EPVOH and Na^+-exchanged MMT resulted in high resistance to dissolution in water, which was ascribed to strong interactions between the components resulting from matching polarities. Annealing the films at 120°C resulted in enhanced resistance to water dissolution and a further reduction in oxygen permeability. © 2015 Wiley Periodicals, Inc. J. Appl. Polym. Sci. **2015**, *132*, 42229.

KEYWORDS: clay; composites; films; packaging; surfaces and interfaces

Received 10 November 2014; accepted 17 March 2015

DOI: 10.1002/app.42229

INTRODUCTION

Ethylene vinyl alcohol (EVOH) copolymers are known for their outstanding gas barrier properties that are superior to other polymers conventionally used in packaging. Their highest oxygen barrier properties have been shown to occur within the range of 27–32 mol % ethylene.[1] However, the poor water solubility of EVOH copolymers at high ethylene content restricts them to use in water-free processes like extrusion coating and blow molding.[1,2] Consequently, water-soluble ethylene-modified copolymers of poly(vinyl alcohol) (EPVOH) have recently been introduced on the market.

Conventional poly(vinyl alcohol) (PVOH) films are hydrophilic and the barrier properties are thus strongly affected by the surrounding relative humidity (RH). For instance, the oxygen permeability of PVOH films in general increases 2500 times when going from 0 to 100% RH.[3] The ethylene modification however gives the polymer a hydrophobic character and the films of EPVOH are stated to have lower oxygen transmission rates (OTR) than standard PVOH films by almost an order of magnitude[4]; they are also more effective barriers at higher relative humidities.[5] These water-soluble EPVOHs are also claimed to have OTR values below that of commercial EVOH coatings (27 mol % ethylene) in the range from 0 to 70% RH.[4] Thus, the water solubility together with favorable barrier properties and approval for food contact give the novel EPVOH grades considerable potential for use as films or coatings for various food packaging applications.

Incorporation of mineral fillers, especially layered silicate minerals like montmorillonite, into polymers is a strategy to form composite materials with improved mechanical strength and barrier properties. Basically, three different structures may arise, namely, (i) phase-separated composites (microcomposites) wherein the layered minerals are present as stacked particles (tactoids), (ii) intercalated nanocomposites where polymer chains are intercalated between the silicate layers forming a well-ordered structure, and (iii) exfoliated nanocomposites where randomly distributed clay layers are dispersed within the polymer in a disordered manner.[6–8] The most widely accepted explanation behind the improved barrier properties is the formation of a more tortuous pathway for permeating molecules, which in turn is related to the diameter of the silicate layers, the extent of delamination of silicate layers, and the orientation of individual sheets within the polymer matrix.[7] A number of other factors which may affect the barrier properties of

Additional Supporting Information may be found in the online version of this article.

hydrophilic polymers by incorporation of layered silicates have been summarized by Xie *et al.*[9] and include reduced hydrophilicity compared to unfilled films; shielding of polymer hydroxyl groups by dispersed clay layers; impact on film morphology like free volume, crystal size, degree of crystallinity, and reduction of macro voids; and formation of strong hydrogen bonds between the polymer and the hydroxyl groups on layered silicates. Even though there are not many easily accessible hydroxyl groups on montmorillonite, such bond formation would act to reduce the diffusion of water molecules through polymer–clay composite films.

Compatibility between polymers and mineral fillers is crucial for the formation of well-dispersed composite structures on the nanoscale and compatibility is gained by matching polarities of the materials.[10,11] Intercalation or exfoliation of the clay particles are favored if the hydrophilicity/hydrophobicity of the polymer and clay are matched.[12] Organophilic modification of clays by exchange of the naturally occurring alkali or alkaline earth metal ions with organic cations can give the clay surfaces a lower surface energy, which may increase their compatibility with a number of hydrophobic polymer matrices.[6,13] These organic modifiers are often cationic alkylammonium or alkylphosphonium surfactants. The presence of bulky alkylammonium ions in the clay interlayer also lead to much higher basal spacing, thus enhancing the potential of polymer intercalation.[6,10,11]

Successful intercalation and exfoliation of hydrophilic hectorite and montmorillonite clays in water-soluble PVOH has been reported, e.g., by Carrado *et al.*,[14] whereas addition of organophilic nanoclays to hydrophilic starch led to the formation of microcomposites.[9,12,15] In contrast, organophilic modified clays have proven to be more effective in promoting intercalated or exfoliated structures in organophilic matrices like polylactide.[16] Natural (unmodified) montmorillonites are easily dispersed in water due to their polar character[11] and are thus compatible with water-soluble polymers like PVOH. The industrially preferred technique to process polymer nanocomposites is the melt intercalation process though solvent mixing and in situ polymerization are also widely adopted methods. Exfoliation in solution has been extensively used for formation of nanocomposites with water-soluble polymers like PVOH.[6]

The presence of polar groups on nonpolar polymers, in some instances, has demonstrated a positive effect on the degree of intercalation with organomodified montmorillonites. Alexandre and Dubois[6] showed that only a low content of polar vinyl acetate groups (from 4.2 mol %) in ethylene–vinyl acetate copolymers was required to favor the formation of intercalation–exfoliation structures, whereas with HDPE only intercalated structures were formed. This study contrasts that herein in that nonpolar "vinyl" groups are present on the polar "hydroxyl" polymer. The investigation of an organoclay in comparison to that of unmodified clays is therefore justified.

In this study, three different bentonite clays were incorporated at selected concentrations in EPVOH. Composite films were solution cast from aqueous dispersions. One of the major objectives was to study how an organophilic, organomodified clay interacts with the hydrophobically modified polymer. The water vapor permeability and oxygen permeability of the composite films at various RHs or after heat treatment were analyzed. Water absorption at different RHs and film dissolution in water were also studied together with thermal properties of the composite films. The distribution of clays was assessed by X-ray diffraction (XRD) and Fourier transform infrared spectroscopy (FTIR).

EXPERIMENTAL

Materials

An EPVOH grade with a degree of hydrolysis (DH) of 97.5–99 mol % and a viscosity of about 25–30 mPas in a 4 wt % water solution at 20°C (determined by a Brookfield synchronized motor rotary type viscometer) was used. The EPVOH is a development product supplied by Kuraray Europe GmbH (Frankfurt a.M., Germany). The product contains <3 wt % methanol and <5 wt % volatiles and was used without further purification. The molecular weight, M_w, was previously determined to be 61,200 g/mol by size exclusion chromatography and the ethylene content was estimated to be about 8.1 mol % by proton NMR analysis.[5] A standard, unmodified PVOH grade with equal viscosity and degree of hydrolysis and with M_w 71,500 g/mol from the same supplier was used as a reference material.

Three different bentonites were used. Cloisite® Na^+ (here denoted Na-MMT) is an unmodified bentonite from Southern Clay Products Inc (Gonzales, TX, USA) with a cation exchange capacity (CEC) of 92.6 meq/100 g clay. The platelets are 1 nm thick with a diameter of 75–100 nm. PGN® is also an unmodified bentonite, from Nanocor (Arlington Heights, IL, USA) which mostly contains Na^+ exchangeable cations but also a small portion of Ca^{2+} (here denoted C-MMT). More significantly, C-MMT has a larger layer diameter of 300–500 nm and a higher CEC value (120 meq/100 g) compared to Na-MMT. Dellite® 67 G is an organically modified bentonite from Laviosa Chimica Mineraria (S.p.A., Livorno, Italy) with CEC of 105 meq/100 g clay and aspect ratio of 500. The majority of the naturally occurring sodium ions have been replaced by dimethyldihydrogenated tallow ammonium ions, $(CH_3)_2N^+(HT)_2$, and the clay is hence denoted Q-MMT, where Q stands for the quaternary ammonium surfactant. Extensive characterization of the bentonites has confirmed the supplier's claims in that they contain more than 95 wt % montmorillonite.

Methods

EPVOH was dissolved in water to a concentration of 10 wt % by holding at 95°C for 60 min under continuous stirring by means of a motorized propeller rotor. The clays were used without pretreatment and polymer–clay composites were formed by addition of 3, 6, 9, or 12 parts dry clay per hundred parts of dry polymer (pph) to the polymer–water mixture while heating. Further addition of water was used to adjust the final concentration of dry matter to 10 wt % in all mixtures.

Film Casting and Evaluation of Film Properties. Films were cast by pouring 10 g polymer–clay dispersions in polystyrene Petri dishes with a diameter of 90 mm, followed by drying to constant weight at 23°C and 50% RH (at least 5 days) until

further treatment or analysis. By keeping the solids content and mass of dispersion transferred to the Petri dish constant, it was possible to form composite films of almost identical thickness, independently of composition. The minor changes in the film density due to the low addition levels of fillers were assumed to have negligible effect on the film properties.

The final film thickness was recorded by a thickness tester (Lorentzen & Wettre type 532 G, Stockholm, Sweden) on at least five locations of each film. The casting method resulted in a film thickness of around 100 μm. In a previous study, it was demonstrated that the barrier properties of EPVOH films reached a plateau value with a film thickness of ca 50 μm[5]; it can therefore be assumed that minor variations in film thickness have a negligible impact on the barrier properties.

Heat treatment is generally utilized to enhance the water resistance of PVOH films since the degree of crystallinity increases almost linearly with the applied temperature during heat treatment.[17] Although annealing can occur above the glass transition temperature of EPVOH (71.8°C), a temperature of 120°C for 10 min was selected for annealing of EPVOH-clay films because this provided the lowest fraction of dissolved matter without inducing any discoloring (yellowing) indicative of degradation.

Water Vapor Transmission Rate. The water vapor transmission rate (WVTR) was measured by the gravimetric cup method (ASTM E96) using silica gel as desiccant. Aluminum cups fitted with sample holders (lids) giving an exposed film area of 50 cm^2 were used. The cups were firmly tightened by placing a rubber O-ring on one side of the film, whereas silicon grease was used to prevent leakage between the film and the aluminum ring on the other side. The cups were placed in a climate chamber (C+10/200, CTS Clima Temperatur Systeme GmbH, Hechingen, Germany) and preconditioned for 24 h prior to analysis of WVTR in an atmosphere of 23°C and 80% RH.

Oxygen Transmission Rate. The oxygen transmission rate (OTR) was measured according to ASTM D3985-05 by a Mocon® OxTran® oxygen transmission rate tester, Model 2/21 (Mocon Inc., Minneapolis, MA, USA), equipped with a coulometric oxygen sensor. An adhesive aluminum foil mask was used to envelop the films, leaving an exposed test area of 5 cm^2. The oxygen concentration in the test gas was 21% and the carrier gas was a blend of 98% nitrogen and 2% hydrogen. Measurements were carried out in duplicates at 23°C and 80% RH under atmospheric pressure. Preconditioning in the test chambers was done for 10 h and measurements were run until steady state was reached.

Moisture Content and Dissolution in Water. The equilibrium moisture content of all films stored at 23°C in an environment of either 50% or 80% RH for at least 24 h were recorded by weighing small pieces cut from each film, followed by drying at 105°C for >1 h (until constant weight; assuming complete removal of water) and subsequent reweighing. Measurements were performed in triplicates. The moisture content was calculated by eq. (1):

$$Moisture\ content = \frac{W_0 - W_d}{W_0} \times 100 \quad (1)$$

where W_0 is the initial weight of the film and W_d is the weight after drying.

The moisture content of the fillers were recorded by storing small portions of each powdered clay for 24 h at 23°C and at two relative humidities: 50 and 80% RH, followed by weighing and drying as above until a constant weight was achieved. The dissolution of films in water is described in the Supporting Information as fraction dissolved matter calculated by eq. (S1).

X-ray Diffraction. X-ray diffraction traces of clay powders and composite films were obtained using a Philips X'Pert Pro diffraction system using a Cu-tube ($\lambda = 1.542$ Å), operating at 40 kV and 40 mA.

Fourier Transform Infrared Spectroscopy. FTIR spectra were collected using a Specac, single pass, attenuated total reflectance Golden Gate™ accessory on a Nicolet, Nexus spectrometer.

Thermal Properties. A modulated differential scanning calorimeter (DSC), Q2000 (TA Instruments, New Castle, DE, USA), was used for studying the thermal properties of polymer films. Film pieces of ~10 mg were placed in Tzero aluminum pans and hermetically sealed. Pure PVOH and EPVOH film pieces were investigated from three replicates of (i) films dried at 23°C and 50% RH; (ii) films with high moisture content (conditioned at 80% RH); and (iii) essentially water-free films (oven dried at 105°C for 90 min). All composite films were analyzed after drying at 23°C and 50% RH and those containing 6 pph clay also after annealing at 120°C. The thermal properties of each clay, as a powder, were also investigated by DSC after drying at 105°C to constant weight for 24 h.

All samples were heated from −20 to 250°C using an oscillating heating rate of 0.32°C/min overlaid on a linear heating rate of 2°C/min. The modulated technique allows heat flow due to heat capacity changes, e.g., glass transitions (reversing heat flow) to be separated from heat flow changes due to kinetic events such as melting, volatilization, and decomposition (i.e., nonreversing heat flow). Glass transition temperatures, T_g, were taken from the inflection point on the reversing heat flow curve, whereas melting temperatures and enthalpies were recorded from the nonreversing heat flow curves.

RESULTS AND DISCUSSION

Film Properties

The cast composite films were visually homogeneous with smooth surfaces and contained no visible particle agglomerates. Incorporation of clays promoted the formation of planar films with no tendency to curl or to separate from the Petri dish at the center of the film. This contrasts with the occasional behavior of the unfilled EPVOH film, in which uneven drying processes caused faster drying regions of the film to separate from the Petri dish while the wet regions remained flat. The presence of the dispersed clay particles introduces physical cross-links into the film structure which act to conserve the dimensional stability of the film. As opposed to covalent bonds being formed

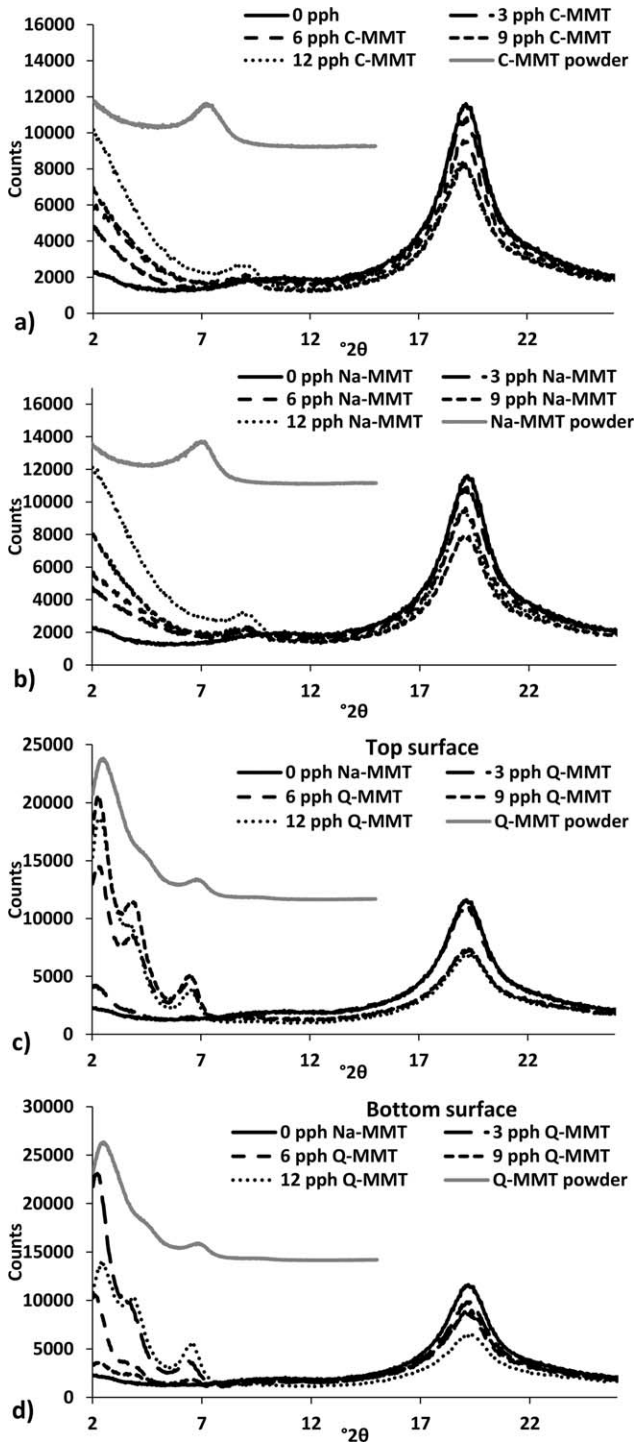

Figure 1. Typical XRD patterns of (a) C-MMT and (b) Na-MMT composite films. In (c) and (d), the XRD patterns of the Q-MMT composite films recorded from the top and bottom surfaces, respectively, are shown. Grey lines show the patterns collected from the clay powders and are offset for clarity.

in conventional cross-linked polymers, the cross-links here occur via physical, often irreversible, strong adsorption processes (van der Waals, hydrogen bonding interactions) between the clay and the polymer. Consequently, the size change upon drying is less pronounced.

Whereas the pure EPVOH films, EPVOH/C-MMT, and EPVOH/Na-MMT composite films remained planar upon additional drying at 105°C, the EPVOH/Q-MMT films curled from the edges toward the center and more so with higher loadings. Partial settling of the Q-MMT particles during initial film preparation, as evidenced by XRD and FTIR and discussed below, may have caused uneven tension in the thickness direction of the films and thus variations in drying rates in the upper and lower portions of the film leading to curling.

The XRD trace for a cast EPVOH film was featureless and rose slightly toward lower angles (Figure 1). The broadness of the peak observed at 19.1°2θ represents the semicrystalline nature of the EPVOH, which is analogous to that of PVOH.[18] Assuming that the crystallinities of all the polymer samples are the same, the intensity of the peak at 19.1°2θ can be used as an internal reference for comparing the intensities of the peaks at low angles (<8°2θ) between samples.

The peak at 6.9°2θ in the traces of the Na-MMT and C-MMT powders is associated with a d_{001} spacing of 12.8 Å. The absence of this peak in the traces obtained from Na-MMT and C-MMT composite films combined with the increasing baseline at angles <5°2θ indicates[19] that the clay in these samples is very well dispersed and disordered, if not exfoliated [Figure 1(a,b)]. The extent of the increasing baseline correlates with the filler loading and is associated with an increasing amount of X-ray scatter due to the nanoscale dispersion of the clay layers. Breen *et al.*[20] also reported the absence of diffraction peaks in PVOH–Cloisite Na^+ nanocomposite films at clay additions below 25 wt %, which was taken as a confirmation of extensively dispersed clay platelets in the polymer matrix. Furthermore, Khairuddin[21] studied adsorption isotherms of PVOH with $M_w \sim 30{,}000$ g/mol on the same clay and XRD analysis indicated the presence of both predominantly intercalated structures with >25 wt % clay and predominantly exfoliated structures with <10 wt % clay. They showed that the d-spacing increased from about 12 Å for untreated clay to about 40 Å at 75 wt % PVOH. The results indicated that PVOH was present in clay galleries as a fully formed bilayer at 25 wt % PVOH and that the amount of PVOH in the interlayer significantly and gradually increased as the amount of PVOH offered rose from 25 to 75 wt %.[22]

It was not possible to unequivocally determine whether the EPVOH was present in the interlayer of Q-MMT. Vaia[19] advised caution when seeking to attribute small increases in basal spacing to the presence of extra material in the interlayer, so the slight shift to lower angles of the d_{001}-spacing from the Q-MMT powder to that in the composite films (2.5–2.23°2θ, respectively) will be disregarded. However, it is very clear that the d_{002} (3.9°2θ) and d_{003} (6.9°2θ) peaks become more prominent and resolved, thus demonstrating improved ordering of the clay layers either in stacks or by the arrangement of stacks in the film. This change could be due to rearrangement/redistribution of the organomodifier, and/or removal of excess modifier from within the interlayer region; all resulting from the extra processing that occurs during the preparation and casting of the EPVOH composite films.

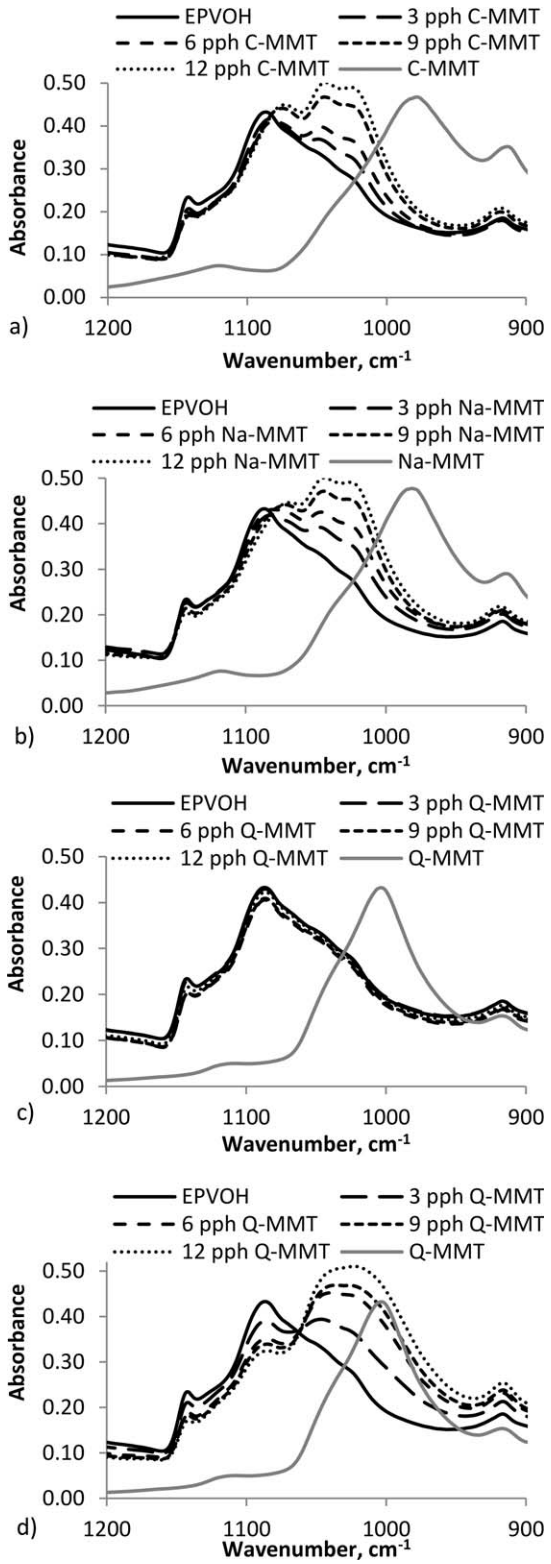

Figure 2. FTIR spectra of (a) C-MMT and (b) Na-MMT composite films. In (c) and (d), the spectra of the Q-MMT composite films recorded from the top and bottom surfaces, respectively, are shown.

The intensities and shapes of the diffraction peaks were very similar from a number of traces collected from the same side and both the top and bottom surfaces of a film sample for all EPVOH composites containing Na-MMT and C-MMT suggesting a homogeneous distribution. However, for the Q-MMT samples, there was no clear correlation between the peak intensity and loading [Figure 1(c,d)]. For example, the trace collected from the top surface of the 3 pph Q-MMT composite indicated a low amount of clay present, whereas that from the bottom surface suggested a higher amount of clay. The differences in peak intensities collected from top and bottom surfaces do indicate settling, i.e., the presence of a graded film structure with a low fraction of Q-MMT at the top surface and a high fraction at the bottom.

FTIR spectra were recorded from both the top and bottom film surfaces to further investigate the film homogeneity. The depth of penetration of the infrared beam is ~2–12 μm, which means only the film in contact with the ATR prism contributes to the FTIR spectrum (total film thickness ~100 μm). For all samples, the spectra collected from each surface at several locations (>6) showed high reproducibility. The pure EPVOH film exhibited a characteristic band at 1085 cm^{-1} representing the C—O stretching in the vinyl alcohol units,[23] whereas bands associated with clay were identified at ~1030 and 1045 cm^{-1} (attributed to the Si—O stretching usually reported in the range of 1150–950 cm^{-1} for montmorillonite)[20,24] (Figure 2). The intensities of the clay bands increased with increasing amounts of C-MMT or Na-MMT and were of similar intensity for both the top and the bottom surfaces, thus suggesting that similar amounts of these clays were present at both surfaces. However, no clay was evident in the top surfaces of the Q-MMT composites as indicated by the lack of clay bands and the spectra being almost identical to that of the pure EPVOH film. In contrast, bands at ~1030 cm^{-1}, which were identified in the spectra recorded from the bottom surface, increased in intensity with increased clay loading. Furthermore, comparison of the relative intensities of the bands at ~1030 cm^{-1} with those at 1085 cm^{-1}, demonstrated that higher amounts of clay were present at the bottom surfaces of the Q-MMT composite films than the corresponding samples containing Na-MMT or C-MMT. The FTIR data thus strongly suggests that Q-MMT partially sediments during the drying stage because of the weak interaction with EPVOH. This weak interaction between Q-MMT and the polymer was also observed by rheology assessments in the wet state.[5] The distribution of different species throughout the films is the topic for an ongoing research study.

Water Vapor Permeability

Figure 3 presents the water vapor barrier properties of EPVOH composites measured at 23°C and 80% RH as water vapor permeability (WVP), in g/Pa·s·m, which accounts for the actual film thickness (100 ± 6 μm for all films), the saturation vapor pressure at the actual test temperature, and the RH gradient across the test films, assuming 0% RH inside the cups. For the EPVOH/Q-MMT composite, a fourfold decrease compared to the unfilled film was achieved by addition of 3 pph Q-MMT. In the case of 3 pph Na-MMT, a significant but lower reduction in WVP was observed, but for 3 pph C-MMT, only a marginal improvement was found. Further addition of any of the clays beyond 3 pph caused the WVP to increase and reach a maximum (at 6 pph for Na-MMT and C-MMT and 9 pph for Q-

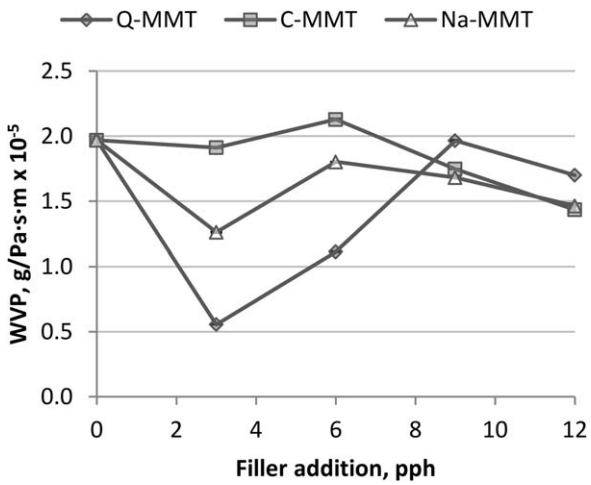

Figure 3. WVP of EPVOH as a function of filler addition at 23°C and 80% RH. Error bars showing standard deviations are included, but smaller than the data markers. The maximum standard deviation was 0.007 × 10^{-5} g/Pa·s·m.

MMT); after the observed maximum, the WVP decreased upon further clay addition.

The WVPs of the composite films are closely related to how the clay is dispersed within. At very low loadings of clay (i.e., 3 pph), the dispersion is likely to be optimized due to a lower probability of physical, direct clay–clay interactions. This presumably leads to the enhanced WVP improvement for Na-MMT and Q-MMT composites at this clay content. At higher clay loadings (>6 pph), the extent of dispersion will be less due to their being insufficient volume within the polymer matrix for the clays to exfoliate; the resulting agglomeration of the clay particles may present channels for water to pass through more readily. Above a certain clay concentration, i.e., the observed maximum, the layers may be combined such that a closely packed and interlocking distribution of the more agglomerated and numerous clay particles results in limiting the passage of water vapor.

The combination of Q-MMT and EPVOH resulted in the lowest overall water vapor permeability (<1.0 g/Pa·s·m × 10^{-5}) at the lowest addition of clay, which supports the creation of a highly impermeable and segregated or self-stratifying clay layer within the film, as indicated by the XRD and FTIR data.

Moisture Content at Equilibrium and Moisture Uptake at Different Relative Humidity

The equilibrium moisture content (eq. (1)) of PVOH and EPVOH films stored at 23°C and 50% RH was about 9.6 and 8.2%, respectively. After exposing the films at 23°C and 80% RH, these values rose to about 15.0 ± 0.4 and 14.8 ± 0.1%, respectively (average from triplicates). Thomas and Stuart[25] showed that equilibrium moisture uptake of PVOH films was reached within <12 h. Supporting Information shows that both film types absorb increasing amounts of moisture as the humidity is increased incrementally from 50% RH, but the increase is slightly higher for PVOH, especially at RH ≥80% (Supporting Information Figure S1). After annealing the PVOH and EPVOH films at 120°C for 10 min, followed by reconditioning at 23°C and 50% RH for 24 h, the average moisture content was about 7 and 6.8%, respectively, indicating that annealing for 10 min causes an apparently permanent reduction of the equilibrium moisture content of the films.

Hodge *et al.*[26] investigated the water absorption of PVOH films and expressed three states in which water can be present; (i) nonfreezing water, i.e., that directly H-bonded to the —OH of PVOH, (ii) freezable water, i.e., that H-bonded to the nonfreezing water, and (iii) free water, i.e., that not perturbed by the H-bonding water associated with PVOH. At the initial stages of water absorption, nonfreezing water disrupts inter- and intramolecular hydrogen bonding within PVOH. While assuming that one nonfreezing water molecule attaches to every —OH group on PVOH (i.e., one H_2O molecule per monomer unit), they concluded that site saturation should be reached at 29 wt % water. Thomas and Stuart[25] also supported the theory of a maximum absorption of nonfreezing water of 29%. Calculations show that the replacement of —OH groups by 8.1 mol % ethylene units reduces the amount of water required to reach site saturation in EPVOH to 26–27% (Supporting Information). The data herein suggests that the amounts of water present in the films are considerably below the level of 22 wt % where freezing water is expected.[26]

The clays are, in addition to the polymers, capable of absorbing moisture from the environment. When changing from 50 to 80% RH, the moisture content in the organomodified clay only increased from about 2 to about 3%, whereas for both C-MMT and Na-MMT, the moisture content was more than doubled (from about 7 to over 15%).

Comparing the equilibrium moisture content in the EPVOH films with those in the hydrophilic C-MMT and Na-MMT clay powders shows that the films contain more bound water at 50% RH (∼8.2% relative to ∼7%), but contain similar amounts at 80% RH (∼15% relative to 15–16%). The presence of clay can influence the size and number of crystallites; the ratio of crystalline to amorphous phases; the free volume; and the connectivity in and between amorphous regions—all of these will influence the amount of sorbed moisture. The specific location of water adsorbed onto clay or EPVOH in composites is difficult to define since when combined, molecular bonding interactions between EPVOH and clay will compete with those between EPVOH and clay with water. This competition, which is dependent on clay/polymer concentrations, will therefore influence the water solubility, the free volume, the amount of water present, and also how strongly it will interact.

The moisture content of the EPVOH/Q-MMT composite films at 23°C and 80% RH decreased linearly ($r^2 = 0.99$) with increased clay concentration from 14.8 with no Q-MMT to 13.2% at 12 pph Q-MMT (Figure 4). For EPVOH/C-MMT and EPVOH/Na-MMT, a slight reduction in moisture content with increased clay load was also observed even though the trends were not as clear as with Q-MMT. The presence of clay will affect polymer folding and larger amounts of clay are supposed to give less crystalline films, but it is not clear whether the observations are related to free volume effects. However, it can

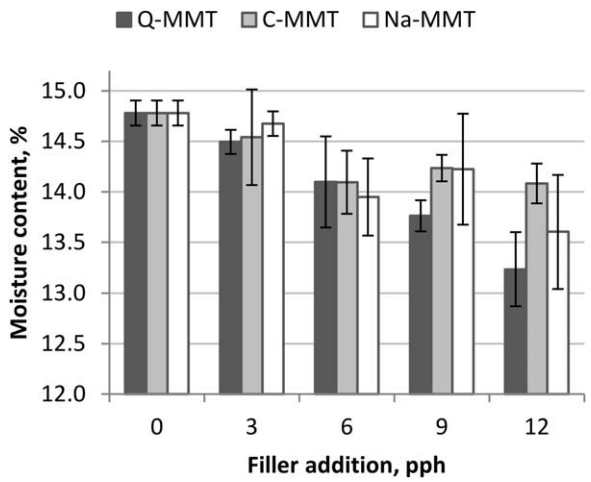

Figure 4. Moisture content in composite films as a function of filler content calculated by eq. (1). Films exposed at 80% RH for 24 h. Average of three measurements. Error bars represent standard deviation.

be asserted that the presence of hydrophilic clays did not lead to increased absorption of moisture in the films when exposed at high RH.

Oxygen Permeability

Figure 5 shows the oxygen permeability (OP) measured at 23°C and 80% RH as an effect of filler addition. The values are expressed in $cm^3 \cdot cm/m^2 \cdot d \cdot bar$, thus taking into account the actual film thickness. Comparative data for OP values of conventional packaging films showed that the OP of unfilled EPVOH at 80% RH was more than two orders of magnitude lower than for LDPE, almost five times lower than for PVOH, and almost identical to the value for PET.[5]

Increasing amounts of C-MMT or Na-MMT in EPVOH resulted in similar linear ($r^2 > 0.98$) decreases as OP reduced from about 2.5 to 1.0 $cm^3 \cdot cm/m^2 \cdot d \cdot bar$ when going from 0 to 12 pph filler.

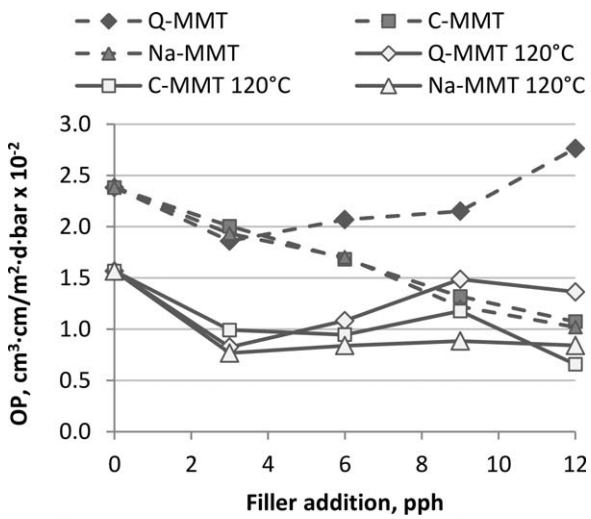

Figure 5. OP of EPVOH films as a function of filler addition (filled symbols), and of annealed films (120°C) (open symbols). Average of two measurements at 23°C and 80% RH with maximum standard deviation of 0.43 (nonannealed) and 0.33 (annealed) $\times 10^{-2}$ $cm^3 \cdot cm/m^2 \cdot d \cdot bar$.

As with the WVP results (Figure 3), Q-MMT showed an optimum OP performance at 3 pph. Although OP slightly increased with addition of 6 and 9 pph, it was still an improvement over the film with no clay. When compared with the other two clays at corresponding addition levels, the incorporation of organophilic clay was effective only at very low addition levels. Despite considerable scattering in data, there is a downward trend in moisture content with increased concentration of C-MMT and Na-MMT (Figure 4). This reduction in moisture, along with the physical barrier properties that the clay constitutes, may explain the improvement in OP with C-MMT and Na-MMT. With Q-MMT, the moisture content substantially decreased with increasing clay content and thus a respective decrease in OP may be expected; however, it was found to act best as a barrier to oxygen at low loadings (3 pph). A distinctly different type of dispersion of Q-MMT (as shown by XRD and FTIR), compared with Na-MMT and C-MMT, due to the limited chemical compatibility between the highly organophilic particles and the less hydrophobic polymer matrix may promote channels for oxygen to proceed through the polymer matrix at higher addition levels.

Figure 5 also shows that annealing the EPVOH film at 120°C for 10 min led to a reduction in OP by a factor of 1.5. Annealed composite films containing 3 pph of any filler resulted in OP values at or below 1.0 $cm^3 \cdot cm/m^2 \cdot d \cdot bar$ equating to a reduced OP by a factor of 2.1–2.5 when compared to the nonannealed films. For annealed films containing C-MMT and Na-MMT, no significant further reduction in OP was observed with increased filler addition, whereas the Q-MMT films expressed a minimum at 3 pph. The OP for Q-MMT films then increased with further filler addition, as observed for the nonannealed films. Here it could be concluded that incorporation of 3 pph of Na-MMT caused a reduction of OP by a factor of 1.2, whereas the combined effect of 3 pph Na-MMT and annealing led to a reduction in OP by a factor of 2.0. Similar summative effects were also achieved with the other two clays, at least at the lowest addition level.

An effect of the annealing process is that the moisture content in the films is reduced, which is one possible mechanism for the observed reduction in OP values. Another possible effect is a change in film crystallinity. This aspect, in combination with effects on dissolution in water as a function of filler addition, is further discussed in Supporting Information (Figure S2).

Comparison Between Experimental Data and Permeability Models

The models based on the formation of a tortuous path for reduction in permeability of polymer composites (P_c) to the permeability of the pure polymer (P_p) proposed by Nielsen in the 1960s and later revised by Cussler and co-workers in the 1980s have proven to be good predictions of P_c/P_p for films with volume fraction of fillers below 10%.[27]

Even though most particle movement will take place in the hydrated prefilm, the comparatively large thickness (~100 μm) of the films in this study should allow the platy clay particles to rotate freely and adopt a random distribution in the films, at least at the lowest concentrations of clay and the lowest aspect ratios of the clay layers. Bharadwaj pointed out that for clay

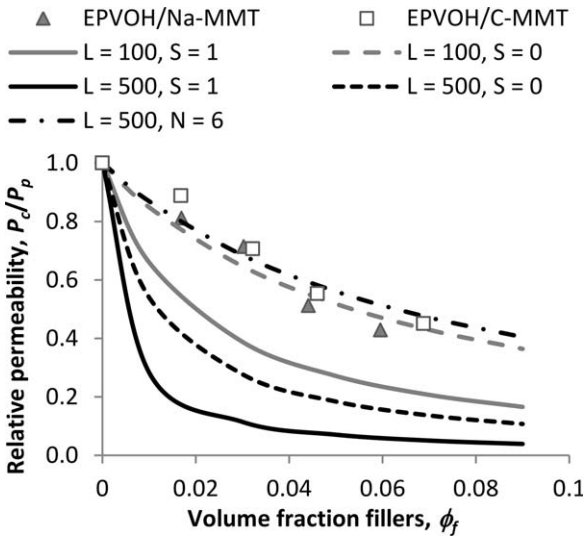

Figure 6. Relative oxygen permeability of EPVOH/Na-MMT and EPVOH/C-MMT composite films with fittings to various models.

particles with large aspect ratio (length > 500 nm), the dependence on the relative orientation of the particles is reduced and a random orientation might be as effective for the barrier properties as alignment perpendicular to the diffusing path, which may ultimately override a lack of complete delamination.[7] A comparison between experimental OP data and values of P_c/P_p predicted by the model proposed by Bharadwaj[7] was undertaken using eq. (2):

$$\frac{P_c}{P_p} = \frac{1-\phi_f}{1+\frac{L}{2W}\phi_f\left(\frac{2}{3}\right)\left(S+\frac{1}{2}\right)} \quad (2)$$

where ϕ_f is the volume fraction of fillers, while L and W are the length and width of the silicate sheets, respectively. S is an order parameter which is equal to zero in case of random orientation of the sheets. When $S = 1$, which corresponds to planar arrangement of sheets (perpendicular to the film surface), eq. (2) is reduced to the equation originally proposed by Nielsen. Figure 6 shows the ratio of oxygen permeability of the Na-MMT and C-MMT composite films to the pure EPVOH film plotted against the volume fraction of fillers, ϕ_f. Since the specific gravity of C-MMT (2.60 g/cm^3) is slightly lower than that of Na-MMT (2.86 g/cm^3), addition of an equal weight fraction of clay implies that C-MMT will occupy a higher volume in the composite, which is illustrated by the marginal shift of ϕ_f to higher values. Also shown are the corresponding relative permeabilities calculated by eq. (2) for the example cases of L set to 100 (Na-MMT) and L set to 500 (C-MMT), respectively, with the order parameter settings $S = 0$ and $S = 1$. The sheet width W was set to 1 nm. For EPVOH/Na-MMT, a perfect match between experimental data and the Bharadwaj model for $S = 0$ was found, which suggest a completely random orientation of the silicate sheets in the film. The higher aspect ratio of C-MMT results in predicted permeability values that are much lower than for Na-MMT. However, experimental data for EPVOH/C-MMT composite films lie close to those for EPVOH/Na-MMT. The model thus indicates that C-MMT is not fully delaminated into homogeneously dispersed layers, which is in contrast to the XRD data which suggested that C-MMT particles are highly disordered, probably exfoliated (Figure 1).

Nazarenko *et al.*[27] concluded that for polystyrene/MMT composites, the oxygen permeability was strictly dependent on the diffusivity, i.e., a pure tortuosity effect, and that the effect of the mineral phase on the solubility was negligible at $\phi_f < 0.1$. However, a smaller reduction in permeability than anticipated by the Nielsen and Cussler models was observed, which was attributed to layer aggregation. They modified the Nielsen model to take into account the presence of homogeneously dispersed, randomly oriented layer stacks (aggregates) with the number N of layers per stack (varying between 3 and 9). Adopting a similar calculation for the EPVOH/C-MMT composite by using $L = 500$ nm, and selecting $N = 6$ allowed a prediction of P_c/P_p that lay very close to the experimental data (Figure 6). An explanation of the mismatch between XRD data and the model fitting could be that C-MMT is present as stacked layers with a highly random orientation or that smearing of the clay layers has occurred. The effect of these processes would not be observable in the X-ray diffraction patterns.

Performing a similar model fitting for EPVOH/Q-MMT suggested the presence of stacks with $N = 9$, 30, and 90 layers for 3, 6, and 9 pph Q-MMT, respectively; hence the aggregate size increased with increased addition of clay. These considerably higher values of N will also reflect that the clay is within concentrated boundaries; recall that the XRD and FTIR data (Figures 1 and 2) show they are not dispersed evenly throughout the film. At 12 pph Q-MMT, the OP was higher for the composite than the pure polymer, which is considered to indicate the occurrence of voids in the polymer matrix due to the presence of large aggregates. It should be noted that due to the considerably lower specific gravity of Q-MMT (1.70 g/cm^3) compared to the values for Na-MMT and C-MMT, the volume occupied by the 3 pph Q-MMT added is as large as for addition of 6 pph Na-MMT or C-MMT ($\phi_f \sim 0.03$) and further so with increased weight loads.

Thermal Properties

Thermal Properties of Polymers. The EPVOH film dried at 105°C for 90 min showed an average T_g of 71.8°C (Figure 7a—labeled Dry), whereas the corresponding value for PVOH was 70.5°C. These figures are close to 72.1°C reported elsewhere for pure PVOH[28] and to the T_g of 72°C for EVOH films with ethylene content of 27 mol %.[2]

Within crystalline domains no water molecules are present, whereas in the amorphous regions pockets of water might exist. Hodge *et al.*[26] showed by DSC that for a water content in the amorphous region of PVOH films below 22 wt %, all water is associated with the polymer as nonfreezing water, i.e., hydrogen-bonded water not possessing sufficient structural order to undergo detectable bulk water phase transitions. Water is an effective plasticizer for PVOH,[17] especially in the form of nonfreezing water.[29] This plasticizing effect is illustrated in Figure 7(a) by a reduction in T_g for EPVOH to 22.9°C when stored at 50% RH (moisture content 8.2%) and to −3.8°C when equilibrated at 80% RH (moisture content 14.8%). The corresponding values for PVOH were 23.8°C and −5.4°C, respectively. Both polymers showed a perfectly linear decrease in

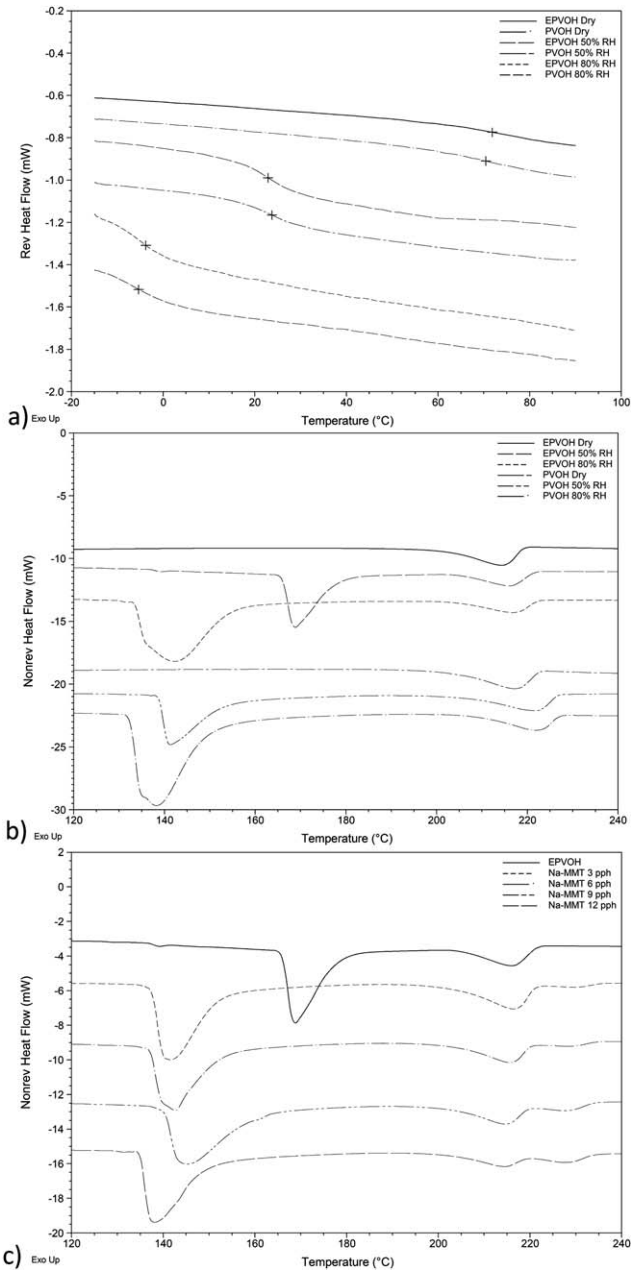

Figure 7. DSC curves for EPVOH and PVOH dry films and films exposed to 50 and 80% RH. (a) Reversing heat flow curves, glass transitions are marked with a cross; (b) nonreversing heat flow curves showing endothermic transitions; (c) nonreversing heat flow curves for EPVOH/Na-MMT composite films conditioned at 23°C and 50% RH.

T_g from the dry state with increasing moisture content ($r^2 = 0.99$). The trend in results are in line with Hodge *et al.*[29] who reported a single glass transition temperature by DMA for each water content of PVOH films with T_g of 30°C at 8 wt % water and T_g of 22°C at 10 wt % water. As mentioned above, the recorded moisture contents at 80% RH in this study are well below the critical 22 wt % level for water to freeze and since MDSC provided no evidence to suggest otherwise, it is assumed that no freezable or free water was present in the samples during these investigations.

Storage and testing of the films at 23°C means that the surrounding temperature is at or close to the T_g of the film when at 50% RH or significantly higher than the T_g of the film at 80% RH. This means that the EPVOH polymer is in the rubbery state in the latter case, i.e., the molecules will have substantially higher mobility thus possibly leading to the formation of a more amorphous structure. It is therefore also more likely that the ingress of water into the polymer will create a path for both water and oxygen molecules to diffuse through the matrix, thus leading to the observed increase in permeability of water vapor and oxygen with increased RH.[5]

The nonreversing heat flow curves presented in Figure 7(b) of the dry EPVOH film showed a melting endothermic event at 214°C with an average melting enthalpy (ΔH_m) of 50 J/g. The corresponding values for dry PVOH were 217°C and 45 J/g, respectively. These figures are comparable to data for PVOH reported elsewhere. For example, Tubbs and Wu[30] reported crystalline melting points in the range of 212–235°C for isotactic PVOH, whereas Mallapragada and Peppas[31] observed melting points in the range of 190–235°C depending on the molecular weight of PVOH; Strawhecker and Manias[32] further identified a bulk T_m of 225°C for a fully hydrolyzed atactic PVOH.

The average values of T_m and ΔH_m for PVOH were 222.1°C and 38.0 J/g (at 50% RH) and 222.4°C and 38.4 J/g (at 80% RH), i.e., a shift to slightly higher melting temperature and lower melting enthalpy compared to the dry film was found, the data was independent of the moisture level. For EPVOH, the corresponding values were 215.3°C and 36.0 J/g (at 50% RH) and 217.6°C and 37.4 J/g (at 80% RH), again the magnitude of the enthalpy changes did not correlate with the moisture content of the films. Annealing the EPVOH film at 120°C for 10 min resulted in a melting enthalpy of 42 J/g which indicates a slightly higher degree of crystallinity compared to the films stored at 23°C and 50 or 80% RH but, as anticipated, a lower crystallinity than in the dry film ($\Delta H_m \sim 50$ J/g).

Strong endothermic transitions were observed between the T_g and T_m events in the nonreversing heat flow curves for both EPVOH and PVOH films when dried at 23°C and conditioned at 50 or 80% RH. Hermetically sealed Tzero pans were used in the MDSC trials and these are designed to suppress volatilization of adsorbed water (in for example polymeric films), a process which normally becomes visible as a broad endotherm centered around 100°C in the nonreversing heat flow curve. Nevertheless, it is believed that the endothermic events observed are due to evaporation of water since these peaks were absent in the MDSC traces for the dry polymer films [Figure 7(b)]. For EPVOH, this transition occurred at an average temperature of 167°C with an average enthalpy of 94.5 J/g when dried at 50% RH [Figure 7(b)], whereas for PVOH, the corresponding endothermic transition occurred at a much lower temperature (142°C) with an enthalpy of 60.2 J/g. After exposure of the films to 80% RH, there was a shift of this endotherm to lower temperature (around 143°C for EPVOH and around 137°C for PVOH) and a simultaneous broadening of the peaks [Figure 7(b)]. The high temperatures at which these endothermic transitions take place indicate that water is very strongly associated

with the polymers. The observations are analogous with Breen *et al.*[20] who found by TG–MS analysis that the temperature over which water was evolved from a pure PVOH film reached a maximum at 140°C. The authors also observed that the peaks became broader and that T_{max} shifted to lower temperature with increased content of water, i.e., reminiscent of the peaks depicted in Figure 7(b).

The enthalpy of the endothermic transitions in the range of 140–170°C increased by a factor of 2–4 (from 94.5 to 233.6 J/g for EPVOH and from 60.2 to 235.2 for PVOH) when comparing films exposed to 80% RH with those exposed to 50% RH, which confirms a strong coupling between this transition and the water content in the films. In addition, the DSC curves shows two overlapping endothermic transitions near 140°C for both PVOH and EPVOH exposed to 80% RH [Figure 7(b)]. This indicates that water is present in at least two different environments within the films, one where the water is more strongly bound to the polymer than the other.

Thermal Properties of Composites. The glass transition temperature increased stepwise from 22.9°C for the pure EPVOH film to 25.5°C with the highest addition level of Q-MMT (12 pph). An increase in T_g has been ascribed to restricted segmental motions due to the presence of the clay[6] since segmental motion is impeded whenever a polymer comes in contact with a surface. From the MDSC experiments, there was no evidence to support that the organomodifier promoted plasticization since the T_g was not reduced, which was observed, for example with organomodified clay (Cloisite® 30B) in poly(acrylated oleic methyl ester).[33] For the Na-MMT and C-MMT composite films, T_g remained similar to that of unfilled EPVOH, which is anticipated since with very well dispersed and highly disordered (or exfoliated) systems fewer restrictive environments will be present to affect segmental mobility.

The T_g after annealing the EPVOH films at 120°C for 10 minutes and reconditioning at 23°C and 50% RH for 24 h was 24.5°C (moisture content 6.8%), which was an increase of 1.6°C compared to the corresponding nonannealed film (8.2% moisture). The composite films containing 6 pph of any of the three fillers (and with less moisture content, 4.9–6.3%) all showed similar T_g values between 24.1 and 25.6°C after annealing and an average upward temperature shift of 1.6–2.4°C.

The weak melting transition (T_m) found in pure EPVOH at about 215°C (at 50% RH) was essentially unaffected by the presence of C-MMT or Na-MMT [exemplified by Na-MMT composite films in Figure 7(c)], whereas the transition took place at a slightly higher temperature (217°C) for all the Q-MMT films. The melting enthalpy of this transition decreased gradually with increased filler content for all clay grades. For Na-MMT [Figure 7(c)], a linear decrease ($r^2 = 0.98$) from 38.0 to 12.5 J/g was observed when going from 3 to 12 pph Na-MMT, which is significantly greater than the minor reduction in the polymer concentration by addition of clay and so reflects a decreased degree of crystallinity of the bulk polymer phase.

The composite films showed the same strong endothermic transitions between T_g and T_m as the pure EPVOH. For Q-MMT composites, an upward shift from 167°C for pure EPVOH to 169–181°C was observed, with a weak trend toward increased temperature with increased amount of clay while the enthalpy moved in the opposite direction (decreasing from 83 to 72 J/g from 3 to 12 pph Q-MMT). For C-MMT, the peak temperature decreased from 162°C (3 pph) to 141°C (12 pph) with an accompanying increase in enthalpy from 95 to 117 J/g. With Na-MMT, the transition was located around 140°C, whereas the enthalpy decreased from 127 to 122 J/g from 3 to 12 pph Na-MMT.

After annealing, there was a downward shift of the first endothermic peak to about 146°C for EPVOH and to 148°C for the 6 pph EPVOH/Q-MMT composite film, with minor changes in enthalpy. In contrast, the temperature at which the transition occurred was unaffected by annealing (within error limits) in the 6 pph C-MMT and Na-MMT composite films. For the latter films, there was however a marked enthalpy reduction from 113 to 79 J/g (C-MMT) and from 124 to 92 J/g (Na-MMT).

The transitions observed in the pure clay minerals (not shown) did not contribute to the traces recorded for the composite films. In addition, the results show that the polymer phase dominates the thermal properties of the composite films and that the fillers did not have any major effect on the overall properties at the different filler levels utilized. Moreover, it could be concluded that the moisture content had greater impact on the glass transition temperature than did the filler concentration.

The endothermic reaction in the mid-range region took place at higher temperatures in the EPVOH and EPVOH/Q-MMT composite films when compared to the Na-MMT and C-MMT composites. In addition, for both C-MMT and Na-MMT, the transition enthalpies increased with filler addition. This difference in thermal behavior raised a question as to whether this transition was solely related to evaporation of water or if it could also be connected with the presence of different types of crystallinity (e.g., crystallite size or form) in the different films. Strawhecker and Manias[34] reported the appearance of a new crystalline form of PVOH with a T_m higher than that of the bulk crystalline form (i.e., >225°C) upon addition of MMT fillers. They observed that the enthalpy of this latter melting transition increased with increased fraction of fillers at the expense of the enthalpy of the bulk-like crystals. In a later study, the same researchers postulated that these new crystals grow around the inorganic fillers and that specific interactions result in a strong adhesion between polymer and fillers.[32] Even though no melting transition could be observed at such high temperatures in this study, a similar effect was observed relating the enthalpies at the two endothermic transitions presented above.

CONCLUSIONS

The combination of Q-MMT and EPVOH resulted in the lowest overall water vapor permeability at 23°C and 80% RH (<1.0 g/Pa·s·m × 10^{-5}) and at low filler additions, thus demonstrating a positive effect of the organophilic Q-MMT clay in reducing the water sensitivity of the polymer. Annealing the EPVOH film at 120°C for 10 min led to a reduction in OP by a factor of 1.5.

Annealed composite films containing 3 pph filler led to OP values at or below 1.0 $cm^3 \cdot cm/m^2 \cdot d \cdot bar$, or a reduced OP by a factor of 2.1–2.5 compared to the nonannealed EPVOH films. Hence, the combined impact of filler addition and annealing was found to promote an effective reduction in the oxygen permeability.

Higher resistance to dissolution in water was observed for composites containing Na-MMT, both for films dried at 23°C and for films annealed at 120°C for 10 min. This is ascribed to strong physical cross-links formed between polymer and clay, which may reduce swelling and hinder dissolution of the composite films in water. An increase in crystallinity resulting from enhanced chain mobility and water loss through the annealing process further contributes to the observed result.

ACKNOWLEDGMENTS

The authors would like to acknowledge Professor Chris Breen for valuable comments on this manuscript.

REFERENCES

1. Leonard, M. W. In The Wiley Encyclopedia of Packaging Technology, 3rd ed.; Yam, K. L., Ed.; Wiley: Hoboken, NJ, **2009**; p 98.
2. Foster, R. H. In The Wiley Encyclopedia of Packaging Technology, 3rd ed. ; Yam, K. L., Ed.; Wiley: Hoboken, NJ, **2009**; p 418.
3. Ashley, R. H. In Polymer Permeability; Comyn, J., Ed.; Elsevier Applied Science Publishers: Essex, UK, **1985**; p 269.
4. Weilbacher, R. In PTS Workshop Innovative Packaging, GV 773; Kleebauer, M.; Sangl, R., Eds; PTS: Munich, 2007; p 6.
5. Johansson, C.; Clegg, F. *J. Appl. Polym. Sci.* **2015**, 132, DOI: 10/1002/APP.41737.
6. Alexandre, M.; Dubois, P. *Mater. Sci. Eng.* **2000**, *28*, 1.
7. Bharadwaj, R. K. *Macromolecules* **2001**, *34*, 9189.
8. McGlashan, S. A.; Halley, P. *J. Polym. Int.* **2003**, *52*, 1767.
9. Xie, F.; Halley, P. J.; Avérous, L. In Nanocomposites with Biodegradable Polymers. Synthesis, Properties and Future Perspectives; Mittal, V., Ed.; Oxford University Press: Oxford, UK, **2011**; p 234.
10. LeBaron, P. C.; Wang, Z.; Pinnavaia, T. *J. Appl. Clay Sci.* **1999**, *15*, 11.
11. Mittal, V. In Nanocomposites with Biodegradable Polymers. Synthesis, Properties and Future Perspectives; Mittal, V., Ed.; Oxford University Press: Oxford, UK, **2011**; p 1.
12. Park, H. M.; Li, X.; Jin, C. Z.; Park, C. Y.; Cho, W. J.; Ha, C. H. *Macromol. Mater. Eng.* **2002**, *287*, 553.
13. Sinha Ray, S.; Bousmina, M. *Prog. Mater. Sci.* **2005**, *50*, 962.
14. Carrado, K. A.; Thyagarajan, P.; Elder, D. W. *Clays Clay Miner.* **1996**, *44*, 506.
15. Chen, B.; Evans, J. R. G. *Carbohydr. Polym.* **2005**, *61*, 455.
16. Paul, M. A.; Alexandre, M.; Degée, P.; Henrist, C.; Rulmont, A.; Dubois, P. *Polymer* **2003**, *44*, 443.
17. Toyoshima, K. In *Polyvinyl Alcohol Properties and Applications*; Finch, C. A., Ed.; Wiley: New York, **1973**; p 339.
18. Assender, H. E.; Windle, A. H. *Polymer* **1998**, *39*, 4295.
19. Vaia, R. A. In Polymer-Clay Nanocomposites; Pinnavaia, T. J.; Beall, G. W., Eds.; John Wiley and Sons: Chichester, England, **2000**; p 245.
20. Breen, A. F.; Breen, C.; Clegg, F.; Döppers, L. M.; Khairuddin,; Labet, M.; Sammon, C.; Yarwood, J. *Polymer* **2012**, *53*, 4420.
21. Khairuddin. Clay-polyvinylalcohol nanocomposites: competitive adsorption of polyvinylalcohol and plasticizers onto Na-bentonite. Ph.D. Thesis. Awarding Body: Sheffield Hallam University, **2012**.
22. Clegg, F.; Breen, C.; Khairuddin., *J. Phys. Chem. B* **2014**, *118*, 13268.
23. Mansur, H.; Sadahira, C. M.; Souza, A. N.; Mansur, A. A. P. *Mater. Sci. Eng. C* **2008**, *28*, 539.
24. Katti, K.; Katti, D. R. *Langmuir* **2006**, *22*, 532.
25. Thomas, P. S.; Stuart, B. H. *Spectrochim. Acta Part A* **1997**, *53*, 2275.
26. Hodge, R. M.; Edward, G.; Simon, G. P. *Polymer* **1996**, *37*, 1371.
27. Nazarenko, S.; Meneghetti, P.; Julmon, P.; Olson, B. G.; Qutubuddin, S. *J. Polym. Sci. Part B: Polym. Phys.* **2007**, *45*, 1733.
28. Nakane, K.; Yamashita, T.; Iwakura, K.; Suzuki, F. *J. Appl. Polym. Sci.* **1999**, *74*, 133.
29. Hodge, R. M.; Bastow, T. J.; Edward, G. H.; Simon, G. P.; Hill, A. *J. Macromolecules* **1996**, *29*, 8137.
30. Tubbs, R. K.; Wu, T. K. In Polyvinyl Alcohol Properties and Applications; Finch, C. A., Ed.; Wiley: New York, **1973**; p 167.
31. Mallapragada, S. K.; Peppas, N. A. *J. Polym. Sci. Part B: Polym. Phys.* **1996**, *34*, 1339.
32. Strawhecker, K. E.; Manias, E. *Macromolecules* **2001**, *34*, 8475.
33. Zhu, L.; Wool, R. P. *Polymer* **2006**, *47*, 8106.
34. Strawhecker, K. E.; Manias, E. *Chem. Mater.* **2000**, *12*, 2943.